

Modifications of expression of genes and proteins involved in DNA repair and nitric oxide metabolism by carbatonides [disodium-2,6-dimethyl-1,4-dihydropyridine-3,5-bis(carboxyloxyacetate) derivatives] in intact and diabetic rats

Kristīne Ošiņa^{1,2}, Elina Leonova^{2,3}, Sergejs Isajevs^{2,3}, Larisa Baumane^{2,3}, Evita Rostoka^{2,3}, Tatjana Sjakste¹, Egils Bisenieks², Gunars Duburs², Brigita Vīgante², and Nikolajs Sjakste^{2,3}

Genomics and Bioinformatics, Institute of Biology of the University of Latvia, Salaspils¹, Latvian Institute of Organic Synthesis², Faculty of Medicine, University of Latvia³, Riga, Latvia

[Received in January 2017; Similarity Check in February 2017; Accepted in August 2017]

Studies on the pathogenesis of *diabetes mellitus* complications indicate that the compounds reducing free radicals and enhancing DNA repair could be prospective as possible remedies. Carbatonides, the disodium-2,6-dimethyl-1,4-dihydropyridine-3,5-bis(carboxyloxyacetate) derivatives, were tested for these properties. EPR spectroscopy showed that metcarbatone was an effective scavenger of hydroxyl radicals produced in the Fenton reaction, etcarbatone, and propcarbatone were less effective, styrylcarbatone was ineffective. UV/VIS spectroscopy revealed that styrylcarbatone manifested a hyperchromic effect when interacting with DNA, while all other carbatonides showed a hypochromic effect. Rats with streptozotocin induced type 1 DM were treated with metcarbatone, etcarbatone or styrylcarbatone (all compounds at doses 0.05 mg kg⁻¹ or 0.5 mg kg⁻¹) nine days after the DM approval. Gene expression levels in kidneys and blood were evaluated by quantitative RT-PCR; protein expression - immunohistochemically in kidneys, heart, sciatic nerve, and eyes; DNA breakage - by comet assay in nucleated blood cells. Induction of DM induced DNA breaks; metcarbatone and styrylcarbatone (low dose) alleviated this effect. Metcarbatone and etcarbatone up-regulated mRNA and protein of eNOS in kidneys of diabetic animals; etcarbatone also in myocardium. Etcarbatone reduced the expression of increased iNOS protein in myocardium, nerve, and kidneys. iNos gene expression was up-regulated in kidneys by etcarbatone and metcarbatone in diabetic animals. In blood, development of DM increased iNos gene expression; etcarbatone and metcarbatone normalised it. Etcarbatone up-regulated the expression of H2AX in kidneys of diabetic animals but decreased the production of c-PARP1. Taken together, our data indicate that carbatonides might have a potential as drugs intended to treat DM complications.

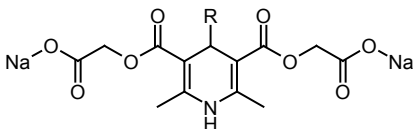
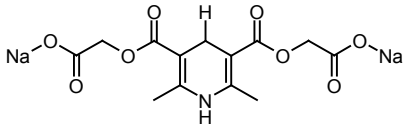
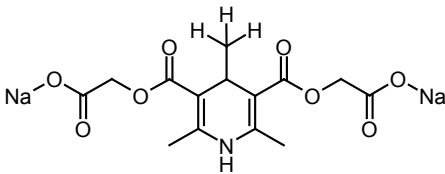
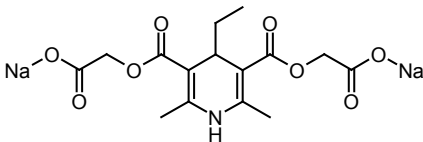
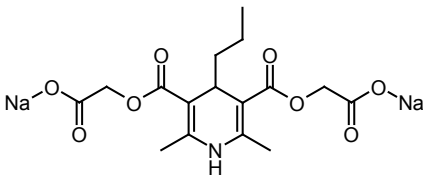
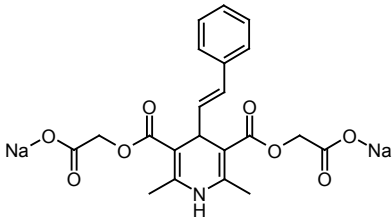
KEY WORDS: 1,4-dihydropyridine derivatives; diabetes mellitus; DNA damage; free radical scavengers; nitric oxide synthases

New remedies for treatment of type one *diabetes mellitus* (T1DM) complications are sought among compounds with antioxidant activities (1, 2). Following this logic, we have chosen some representatives of group of 1,4-dihydropyridine (1,4-DHP) derivatives synthesised in the Latvian Institute of Organic Synthesis (see Table 1 for structures). These compounds did not manifest high Ca²⁺-channel blocker activity (3), however, they displayed antioxidant activities (4) and interfered with mitochondria by uncoupling respiration and phosphorylation (5). Some of these compounds manifested antidiabetic activities. For example, cerebrocrast promoted decrease of food intake (6), protected pancreatic cells from streptozotocin (STZ)-

induced damage and reduced glucose level in blood of animals with developed DM (7, 8), and acted synergistically with insulin on heart functions and metabolism in diabetic rats (9). The same 1,4-DHP derivative and its analogues normalised nitric oxide (NO) production in diabetic animals and modified expression of genes involved in NO metabolism (10). Besides its antioxidant properties, 1,4-DHP derivative AV-153 turns out to be a DNA repair enhancer (11) capable of interacting directly with DNA (12); cerebrocrast and its analogues manifest identical properties (10). We have shown that AV-153 down-regulates poly(ADP)ribose polymerase 1 (PARP1) and inducible NO synthase (iNOS) protein expression and increases the level of endothelial NO synthase (eNOS) protein and H2A histone family member X (*H2afx*) gene expression in kidneys of animals with experimental DM (13). Several 1,4-DHPs modify expression of proteasomal genes (14). Taken

Correspondence to: Kristīne Ošiņa, Institute of Biology of the University of Latvia, Miera Street 3, Salaspils, LV 2169, Latvia, phone +371 67944988, fax +37167944988, E-mail:kristine.osina@lu.lv

Table 1 Chemical structures of carbatonides [disodium-2,6-dimethyl-1,4-dihydropyridine-3,5-bis(carbonyloxyacetate) derivatives]

Compound	R	Formula	Chemical name
			
Carbatone	H		Disodium 2,6-dimethyl-1,4-dihydropyridin-3,5-bis-carbonyloxyacetate
Metcarbatone	CH ₃		Disodium 2,4,6-trimethyl-1,4-dihydropyridin-3,5-bis-carbonyloxyacetate
Etcarbatone	C ₂ H ₅		Disodium 4-ethyl-2, 6-dimethyl-1,4-dihydropyridin-3,5-bis-carbonyloxyacetate
Propcarbatone	C ₃ H ₄ -n		Disodium 2,6-dimethyl-4-(n-propyl)-1,4-dihydropyridin-3,5-bis-carbonyloxyacetate
Styrylcarbatone	-CH=CH-C ₆ H ₅		Disodium 2,6-dimethyl-4-styryl-1,4-dihydropyridin-3,5-bis-carbonyloxyacetate

together, this group of 1,4-DHP derivatives appeared to be prospective for the study of their possible application as remedies against DM complications and should be studied further.

The aim of the present work was to test disodium-2,6-dimethyl-1,4-dihydropyridine-3,5-bis(carbonyloxyacetate) derivatives (carbatonides) with different groups in position 4 by means of EPR spectroscopy for its capability to scavenge hydroxyl radical produced in the Fenton reaction, to protect DNA against above mentioned radicals *in vitro*, and to bind DNA. A series of *in vivo* experiments were conducted to study mRNA and protein expression levels in healthy animals and the expression of several proteins and genes involved in apoptosis, DNA repair, and free radical production in animals with STZ-induced *diabetes mellitus*. It is considered that impaired production of NO is a crucial point in development of DM complications. It is mainly due to the uncoupling of eNOS and overexpression of iNOS, as well as increased NO synthase-independent generation

of NO by xanthine dehydrogenase (XDH) (10, 13 and references therein). This determined the choice of the abovementioned genes. Generation of DNA lesions and impaired DNA repair is also an important step in the pathogenesis of DM complications. The level of poly(ADP) ribose synthesis by PARPs characterises the intensity of the repair response to DNA lesions. This determined the choice of the PARP1 gene and protein study; moreover, the cleaved form of the protein is a sensitive apoptosis marker. H2AX histone, a sensitive marker of DNA double strand breaks, was chosen also to characterise the level of DNA lesions (13 and references therein).

MATERIALS AND METHODS

Chemicals

Carbatone, metcarbatone, etcarbatone, propcarbatone, and styrylcarbatone (J-9-125) (Table 1) were synthesised

at the Latvian Institute of Organic Synthesis and characterised by usual physico-chemical methods: $^1\text{H-NMR}$, $^{13}\text{C-NMR}$, IR spectroscopy, as well as LC-MS and elemental analysis. STZ, citric acid, EDTA, ferrous sulphate, hydrogen peroxide, low-melting agarose, NaCl, NaOH, Tris base, 5,5-dimethylpyrroline-N-oxide, ethidium bromide, and TRI reagent were purchased from Sigma-Aldrich Chemie (Taufkirchen, Germany).

In vitro experiments

Fenton reaction – ESR measurements

Trapping of the hydroxyl radical was performed by 5,5-dimethylpyrroline-N-oxide (DMPO)-spin trap. EPR spectra of the spin trap and radical complex were recorded at room temperature using a Bruker D-200 ER spectrometer (IBM Bruker Ltd, Coventry, UK), operating at X-band with a TM cavity and capillary tube. For the Fenton reaction ($\text{Fe}^{2+} + \text{H}_2\text{O}_2 \rightarrow \text{Fe}^{3+} + \bullet\text{OH} + \text{OH}^-$), reactants containing 80 mmol L $^{-1}$ DMPO, 250 $\mu\text{mol L}^{-1}$ ferrous sulphate, 250 $\mu\text{mol L}^{-1}$ H $_2\text{O}_2$ and 20 μL of 1,4-DHP were mixed in a test tube to a final volume of 100 μL and the reaction mixture was then transferred to a capillary tube for the measurement of the EPR signal. The EPR spectrometer settings were as follows: modulation frequency – 100 kHz; X band microwave frequency – 9.5 GHz; microwave power 0–15 mW (milliwatts); modulation amplitude – 1.0 G (gauss); time constant – 160 s; scan time – 200 s, and receiver gain – 1×10^5 (15).

UV/VIS spectroscopic measurements and fluorescence assays

UV-VIS spectra of the tested compounds were recorded on a Perkin Elmer Lambda 25 UV/VIS spectrophotometer in the absence of DNA and presence of increasing amounts of DNA in 5 mmol L $^{-1}$ NaCl and 5 mmol L $^{-1}$ Tris HCl at pH 7. The solution of the tested compound (25 $\mu\text{mol L}^{-1}$) was diluted out of 1 mmol L $^{-1}$ stock solution in the buffer in a quartz cell (1 mL). The reference cell was filled with 1 mL of buffer. The mixture was mixed thoroughly and titrated with 7.48 mmol L $^{-1}$ of sonicated pTZ57R plasmid DNA solution, 5 μL each time to both sample and reference cells. Spectra were recorded in 400–200 nm interval at room temperature (10). Spectrofluorimetric analyses were performed on a Fluoromax-3 (Horiba JOBIN YVON, Edison, NJ, USA) device. The fluorescence spectra of 25 $\mu\text{mol L}^{-1}$ solution of compounds in 50 mmol L $^{-1}$ NaCl and 5 mmol L $^{-1}$ Tris HCl at pH 7 were recorded in the range of 365–600 nm at excitation wavelength of 350 nm or 360 nm. DNA concentration was increased by 12.5 μmol at each step until saturation was obtained in fluorescence spectroscopic experiments on ethidium bromide extrusion from complex with DNA. The complex of plasmid DNA (74.8 $\mu\text{mol L}^{-1}$) and ethidium bromide (1.26 $\mu\text{mol L}^{-1}$) was titrated with 8.3 $\mu\text{mol L}^{-1}$ aliquots of 2.5 mmol L $^{-1}$ solution

of the compound. Measurements were carried out at room temperature in 50 mmol L $^{-1}$ NaCl and 5 mmol L $^{-1}$ Tris HCl at pH 7 using 1 cm cuvette. Excitation wavelength was 335 nm, fluorescence was measured at 600 nm. Binding constants were calculated as described (10, 12).

In vivo experiments

Animals

This study was approved by the Animal Ethics Committee of the Food and Veterinary Service (Riga, Latvia) and it was carried out according to the guidelines of the Directive 86/609/EEC “European Convention for the Protection of Vertebrate Animals Used for Experimental and other Scientific Purposes” (1986). Wistar male rats (215.0 \pm 5.6 g) were purchased from the Laboratory of Experimental Animals, Riga Stradins University, Riga, Latvia. Animals were kept at a temperature of 22 \pm 0.5 $^\circ\text{C}$ with a 12-h light/dark cycle and fed with a standard laboratory diet.

Experiment design

In total, 128 rats were used in the study. T1DM was induced by STZ injection via the tail vein (50 mg kg $^{-1}$, freshly dissolved in 10 mmol L $^{-1}$ citrate buffer, pH 4.5, injection volume 0.2–0.25 mL). Control rats received 0.2 mL of 0.9 % NaCl via the tail vein. Diabetes was certified by measuring glucose level in tail vein blood of the fed rats in the morning 48 hours after the induction using a portable glucometer MediSense OptiumXceed (Abbott Diagnostics Ltd, Maidenhead, UK). Animals with blood glucose >13.89 mmol L $^{-1}$ (250 mg dL $^{-1}$) were used in experiments. The experiment was performed at day nine after confirmation of DM. Rats were divided in two big groups: control group (animals without DM) and STZ group (animals with induced DM). Each group was divided in seven subgroups: animals with no treatment, animals treated with either metcarbatone at low dose (0.05 mg kg $^{-1}$ *p.o.* of metcarbatone for three days), metcarbatone at high dose (0.5 mg kg $^{-1}$, similarly), etcarbatone at low dose, etcarbatone at high dose, styrylcarbatone at low dose or styrylcarbatone at high dose. Each group contained at least three animals. After the treatment course glucose was measured, then the rats were euthanised, kidney and blood samples of all animals were taken and frozen in liquid nitrogen for RNA extraction. Samples of heart, kidneys, eyes and sciatic nerve of animals in groups of untreated animals and animals treated with metcarbatone and etcarbatone were fixed for immunochemistry.

Tissue processing and immunohistochemical examination

Rat kidney, heart, eye and sciatic nerve tissue specimens were processed and examined essentially as described (10). Tissue specimens were fixed in 10 % neutral buffered formalin and embedded in paraffin. Specimens were cut in

5 µm thick section on a rotary microtome and mounted on poly-lysine coated glass slide. The following antibodies were used: rabbit polyclonal eNOS antibody (AbCam, Cambridge, UK, ab 66127; dilution 1:100), rabbit polyclonal iNOS antibody (AbCam, ab 3523; dilution 1:200), anti-cleaved PARP1 rabbit monoclonal antibody (AbCam, ab32651, dilution 1:200), and rabbit polyclonal histone gamma-H2AX antibody (AbCam, ab11175, dilution 1:500). Bound antibodies were detected using the EnVision (DAKO, Glostrup, Denmark) reagent (30 min at room temperature). The immunoperoxidase reaction colour was developed by incubating the slides with diaminobenzidine for 7 min. Each experiment included a negative control (mice tissues) omitting the primary antibody and positive controls (human tissues) - lung tissue and liver tissues for iNOS, liver and aorta tissues for eNOS and thyroid papillary carcinoma tissue for cleaved PARP1 and histone H2AX.

Gene expression studies

Gene expression studies were performed as described (10). Total RNA was isolated from kidneys and blood using TRI reagent and purified using DNA-free kit (Ambion, Austin, TX, USA). RNA quantity and purity were determined by spectrophotometry. The integrity of RNAs was monitored by gel electrophoresis and only specimens with well-pronounced rRNA bands were taken for reactions. To obtain cDNA, 2 µg of RNA were reverse-transcribed using a random hexamer primer (RevertAid™ First Strand Synthesis Kit, Fermentas, Vilnius, Lithuania) (10). Primer sequences for *iNos* gene were 5'-GCTACACTTCCAACGCAACA-3' (forward primer) and 5'-CATGGTGAACACGTTCTTGG-3' (reverse primer). Primers for *eNos* gene were 5'-GAACCTGAGGGTGCCAG-3' (forward primer) and 5'-TCCGATTCAACAGTGTCTCCT-3' (reverse primer). Primers for *Parp1* gene were 5'-CGGAGAGGCTTTACCGAGTG-3' (forward primer) and 5'-GAACATGGGTGACTGCACCA-3' (reverse primer). Primers for *H2afx* gene were 5'-CGGTTTGTCTCCTGGCGTTT-3' (forward primer) and 5'-ACATCGTGTGCGAGGTAGAA-3' (reverse primer). Primers for xanthine deoxygenase gene *Xdh* were 5'-CGGACCCTGAAACAACACTT-3' (forward primer) and 5'-CAAGCAGGCATTGACAGAAA-3' (reverse primer). RNA-polymerase II (5'-GCCAGAGTCTCCCATGTGTT-3' and 5'-GTCGGTGGACTCTGTTTGT-3', 135 bp) was chosen as a reference gene.

SYBR® Green PCR Master Mix (Applied Biosystems, Foster City, CA, USA) was used for determination of gene expression. Amplification and detection of specific products were performed on a StepOne™ Real-Time PCR System (Applied Biosystems, Foster City, CA, USA) using the following temperature-time profile: one cycle of 95 °C for 10 min, and 40 cycles of 95 °C for 15 sec, 60 °C for 1 min.

To check the specificity of the amplification products, the dissociation curve mode was used (one cycle at 95 °C for 15 sec, 60 °C for 1 min, and 95 °C for 15 sec).

The single cell gel electrophoresis (comet assay)

The comet assay was performed as described (11, 16) with minor modifications (17). Blood for the comet assay was taken from the tail vein into a plastic capillary with heparin (Microvette CB 300, Sarstedt, Germany). Next, 10 µL of fresh heparinised blood were mixed with 120 µL of prewarmed (37 °C) 1 % low-melting agarose, 100 µL of the mixture were placed on a microscope slide that had been pre-coated with 0.5 % normal melting-point agarose. The cell membranes were lysed by keeping the slides in a cold lysing solution (pH 10.0) that contained 2.5 mol L⁻¹ NaCl, 10 mmol L⁻¹ Na₂EDTA, 10 mmol L⁻¹ Tris, 1 % Triton-X 100, 5 % DMSO (Sigma-Aldrich, Germany), for at least 1 h. Subsequently, the slides were placed in a horizontal tank filled with fresh electrophoresis buffer (1 mmol L⁻¹ Na₂EDTA, 300 mmol L⁻¹ NaOH, pH 13.2) for 20 min to allow DNA to unwind. Then, horizontal electrophoresis was carried out for 20 min at 300 mA, 1 V cm⁻¹ and 4 °C. After electrophoresis, slides were washed twice for 5 min with 0.4 mol L⁻¹ Tris buffer (pH 7.5) for neutralisation and then fixed in ice-cold 96 % ethanol for 10 min. Slides were dried and stained with ethidium bromide and analysed with a fluorescence microscope equipped with 515–560 nm excitation filter and 590 nm barrier filter. Cells were visually graded into five classes (A₀–A₄) (11) from class 0 (undamaged, no discernible tail) to class 4 (almost all DNA in tail, insignificant head). The mean value of DNA damage (D) in arbitrary units was calculated as follows: $D = A_1 + 2 \times A_2 + 3 \times A_3 + 4 \times A_4$.

Statistics

GraphPad Prism 6 software (San Diego, CA, USA) was used for statistical analysis. Results of the immunohistochemical data, real time PCR, and comet assay were analysed by an unpaired t test with Welch's correction and two-way ANOVA followed by Dunnett's multiple comparisons test. Data are presented as means±SEM.

RESULTS

Radical scavenging - EPR measurements

The ability of the 1,4-DHPs to scavenge the OH radical produced in the Fenton reaction was tested by the ESR method. The signals of the second compound of EPR spectra were measured on the 3rd (I₃) and 5th min (I₅) and the difference between them I₃ - I₅ was calculated (Fig. 1; A). The scavengers of OH radicals should increase the difference between I₃ and I₅. Representative kinetics of the decrease in the EPR signal intensity is shown in Figure 1B. Compounds were given at 1 mmol L⁻¹ concentration.

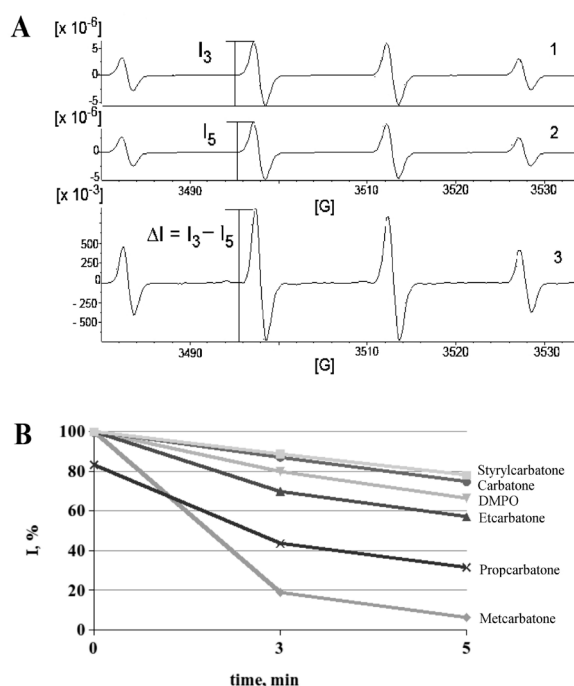


Figure 1 A - EPR spectra of DMPO-OH radicals generated in the Fenton reaction in presence of DMPO. 1 - EPR spectra of DMPO-OH radicals 3 min after mixing the components for the Fenton reaction. 2 - EPR spectra of DMPO-OH radicals 5 min after mixing the components for the Fenton reaction. I_3 and I_5 - intensities of EPR signals used for the quantification of DMPO-OH radicals in the corresponding time. 3 - difference between 3 min and 5 min spectra indicating a decrease in the signal intensity and lack of generation of other radicals. B - time of decrease in the intensity of DMPO-OH radical spectra, percent compared to the initial point

Carbatone did not scavenge the hydroxyl radical produced in the Fenton reaction, metcarbatone was an effective scavenger (radical concentration decreased up to 31.4 % compared to the control, DMPO alone). Etcabatone was less effective (up to 98.3 %); efficiency of propcarbatone was better than that of etcabatone (86.4 %), but worse compared to metcarbatone. The scavenging efficiency of metcarbatone was dependent on the concentration: 0.5 mmol L⁻¹ decreased the radical concentration up to 84.4 % of the radical; when given at concentrations 0.2 or 0.1 mmol L⁻¹ the compound was not effective (not shown). Styrylcarbatone even favoured the radicals' generation up to 106 %.

DNA binding

The UV/VIS spectra of carbatone and propcarbatone are given in Figure 2, panel A. Other spectra are not shown. All the carbatonides absorbed light in the UV part of spectrum with a maximum at 235 nm and in the visible part of spectrum with a maximum at 380 nm for carbatone and at 355 nm for other carbatonides. In the UV/VIS titration assay carbatone, metcarbatone, etcabatone, and propcarbatone manifested a slight hypochromic effect when interacting with DNA. Binding constants were 1.09×10^2

for carbatone, 0.82×10^2 for metcarbatone, 0.54×10^2 for etcabatone, and 1.11×10^2 for propcarbatone. Unlike other carbatonides, styrylcarbatone manifested a hyperchromic effect in the presence of DNA (not shown), its affinity to DNA was higher compared to other carbatonides ($K=1.9 \times 10^3$ L mol⁻¹). When irradiated with excitation light at 360 nm, all five compounds emitted fluorescence with a maximum at 450 nm. Interestingly, in the presence of DNA, fluorescence of carbatone and propcarbatone (not shown) was increased; on the contrary, DNA quenched fluorescence of metcarbatone (not shown), etcabatone and styrylcarbatone (Stern-Volmer quenching constants were 3.8×10^2 L mol⁻¹, 9.5×10^2 L mol⁻¹ and 1.4×10^4 L mol⁻¹, respectively; Figure 2, panel B). Styrylcarbatone intercalates the DNA molecule as it effectively decreased fluorescence of $74.8 \mu\text{mol L}^{-1}$ DNA and $1.26 \mu\text{mol L}^{-1}$ ethidium bromide complex - up to 70 % after 16 additions of $10 \mu\text{mol L}^{-1}$ of the compound to the complex (Figure 2, panel C).

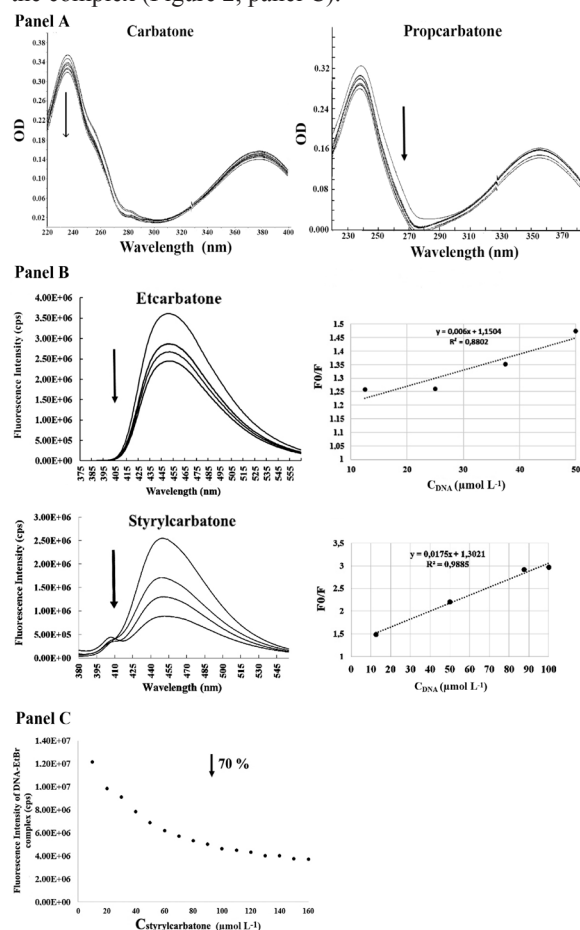


Figure 2 DNA binding of assays. (Panel A) UV/VIS spectroscopy. Plasmid DNA solution, $10 \mu\text{mol L}^{-1}$ each time, was added to both sample and reference cells. (Panel B) Fluorescence spectra of carbatonides with excitation at $\lambda=360$ nm (etcabatone) and $\lambda=350$ nm (styrylcarbatone) in absence and presence of different concentrations of sonicated pTZ57R plasmid DNA. Carbatonide concentration was $25 \mu\text{mol L}^{-1}$, DNA concentration was increased by $12.5 \mu\text{mol L}^{-1}$ at each step until saturation. (Panel C) Fluorescence quenching plot of the ethidium bromide-pTZ57R plasmid DNA complex as a function of styrylcarbatone concentration

Gene and protein expression studies

Styrylcarbatone, metcarbatone, and etcarbatone were chosen for the *in vivo* studies. These compounds did not produce the hypoglycaemic effect (not shown). The impact of these compounds on the expression of several genes and proteins involved in NO production and DNA repair were tested in the kidneys of normal and diabetic animals. The expression of genes was also monitored in blood samples. Besides kidneys, immunohistochemical studies were performed also on heart, nerve, and eye tissues.

The expression of the *Parp1* gene (a marker of DNA repair), cleaved PARP1 protein (a marker of apoptosis), both proteins and genes of histone H2AX (DNA breakage marker) and two NO synthases (iNOS and eNOS) as well as *Xdh* gene (NO producing enzyme), were monitored. The quantified data of immunohistochemistry and real time PCR for kidneys are given in Tables 2-5.

Parp1 gene

We could not detect any significant differences in *Parp1* gene expression in kidneys of intact rats and animals with STZ *diabetes mellitus* (Table 2). However, the administration of styrylcarbatone, etcarbatone, and metcarbatone at both doses caused a highly significant more than two-fold increase ($P<0.001$) of the *Parp1* gene expression in kidneys of intact animals. When administered to diabetic animals, all the three compounds, except etcarbatone at high dose, also caused a strong increase in the gene expression ($P<0.01$).

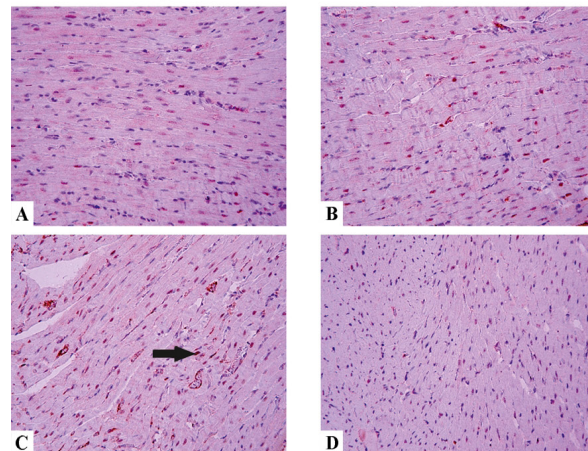
In blood cells, diabetes induction was followed by a strong, almost two-fold, increase in *Parp1* gene expression ($P=0.003$). Both doses of etcarbatone attenuated the increase ($P<0.001$). However, styrylcarbatone and metcarbatone were not effective (Table 2).

Cleaved PARP1 (c-PARP1) protein

Development of the STZ-induced *diabetes mellitus* significantly increased the number of cells positive for c-PARP1 protein, a marker of apoptosis, in kidney tissue ($P=0.004$). Metcarbatone did not modify the expression of the enzyme in diabetic kidneys, while administration of etcarbatone at both doses decreased the number of cells positive for c-PARP1 in diabetic kidneys ($P<0.001$), although the compound upregulated the expression of the protein in kidneys of intact animals ($P<0.05$) (Table 3).

In heart tissues, c-PARP1 was detected in cardiomyocytes, in some inflammatory interstitial cells, and around blood vessels (Figure 3). Development of *diabetes mellitus* caused a three-fold increase in the cells positive for c-PARP1 protein in myocardium ($P=0.025$). The number of apoptotic cells was normalised by etcarbatone at both doses ($P<0.01$) and low dose of metcarbatone ($P=0.018$). In the sciatic nerve, the c-PARP1 protein was noticed in Schwann's cells and in the inflammatory cells around nerve sheaths (not shown). The three-fold increase ($P=0.009$) in

c-PARP1, myocardium



H2AX, kidney

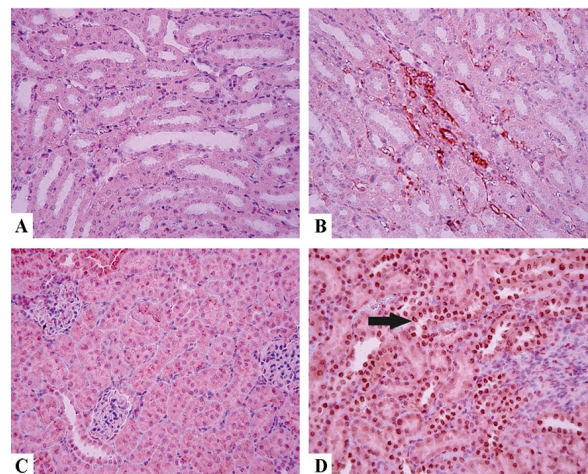


Figure 3 Tissue distribution of apoptosis and DNA breakage markers. Upper panel: c-PARP1 expression in the myocardium. Immunohistochemical staining method, magnification $\times 200$. A - control, B - etcarbatone at 0.05 mg kg^{-1} , C - STZ (streptozotocin), D - STZ+etcarbatone at 0.05 mg kg^{-1} . Arrow indicates positively stained cells. Lower panel: H2AX expression in the kidney tissue. Immunohistochemical staining method, magnification $\times 200$. A - control, B - etcarbatone at 0.05 mg kg^{-1} , C - STZ, D - STZ+etcarbatone at 0.05 mg kg^{-1} . Arrow indicates positively stained cells

the number of cells positive for this apoptotic protein following DM development was normalised by etcarbatone at both doses ($P<0.001$); metcarbatone did not produce any impact on the number of apoptotic cells. In eye tissues, there was also a three-fold increase ($P=0.005$) of c-PARP1 positive cells after induction of diabetes; both doses of etcarbatone increased it even more ($P<0.001$) but metcarbatone showed no effect (Table 3).

Histone H2AX and H2afx gene

Numerical data are presented in Tables 2 and 3, microphotographs – in Figure 3. In kidneys, expression of H2AX was observed in proximal and distal canaliculi, in glomeruli, and blood vessel walls (Figure 3). The expression of this marker of DNA breakage on gene level did not

Table 2 Effects of carbatonides on expression of *Parp1* and *H2afx* genes in kidneys and blood of control and diabetic rats

	Kidneys <i>Parp1</i>	Kidneys <i>H2afx</i>	Blood <i>Parp1</i>	Blood <i>H2afx</i>
Control	0.68 ± 0.05 n=11	0.20 ± 0.02 n=11	0.055 ± 0.007 n=10	0.034 ± 0.006 n=12
STZ	0.63 ± 0.04 n=9	0.21 ± 0.02 n=11	0.089 ± 0.010 n=15*	0.056 ± 0.007 n=15*
Metcarbatone 0.05 mg kg ⁻¹	1.27 ± 0.19 n=4***	0.19 ± 0.02 n=4	0.032 ± 0.009 n=4	0.027 ± 0.006 n=4
Metcarbatone 0.5 mg kg ⁻¹	1.19 ± 0.05 n=4***	0.21 ± 0.02 n=4	0.023 ± 0.002 n=4	0.019 ± 0.001 n=4
Metcarbatone 0.05 mg kg ⁻¹ + STZ	1.42 ± 0.09 n=5###	0.21 ± 0.01 n=5	0.093 ± 0.022 n=4	0.041 ± 0.006 n=4
Metcarbatone 0.5 mg kg ⁻¹ + STZ	1.55 ± 0.16 n=5###	0.25 ± 0.01 n=5	0.086 ± 0.017 n=5	0.039 ± 0.008 n=5
Etcabatone 0.05 mg kg ⁻¹	1.67 ± 0.28 n=3***	0.24 ± 0.04 n=3	0.023 ± 0.004 n=3	0.021 ± 0.001 n=3
Etcabatone 0.5 mg kg ⁻¹	1.59 ± 0.07 n=4***	0.20 ± 0.02 n=4	0.036 ± 0.002 n=4	0.024 ± 0.007 n=4
Etcabatone 0.05 mg kg ⁻¹ + STZ	0.99 ± 0.08 n=5##	0.24 ± 0.03 n=5	0.036 ± 0.009 n=5##	0.034 ± 0.006 n=5#
Etcabatone 0.5 mg kg ⁻¹ + STZ	0.85 ± 0.10 n=5	0.18 ± 0.02 n=5	0.033 ± 0.004 n=5###	0.029 ± 0.003 n=5#
Styrylcarbatone 0.05 mg kg ⁻¹	1.45 ± 0.16 n=4***	0.24 ± 0.02 n=4	0.062 ± 0.017 n=4	0.033 ± 0.007 n=4
Styrylcarbatone 0.5 mg kg ⁻¹	1.72 ± 0.39 n=4***	0.28 ± 0.09 n=4	0.055 ± 0.010 n=3	0.037 ± 0.008 n=3
Styrylcarbatone 0.05 mg kg ⁻¹ + STZ	1.53 ± 0.18 n=5###	0.18 ± 0.02 n=5	0.069 ± 0.013 n=5	0.034 ± 0.006 n=5
Styrylcarbatone 0.5 mg kg ⁻¹ + STZ	2.37 ± 0.11 n=5###	0.28 ± 0.02 n=5	0.110 ± 0.022 n=4	0.049 ± 0.009 n=4

STZ – streptozotocin. Values are represented as the mean ± SEM. **p*<0.05; ***p*<0.01; ****p*<0.001 vs. Control. #*p*<0.05; ##*p*<0.01; ###*p*<0.001 vs. STZ

change in the kidneys of animals in any group, however, etcabatone treatment at both doses up-regulated protein expression in diabetic animals (*P*<0.01, Table 3). In diabetic animals, gene expression increased in blood (*P*=0.002); etcabatone at both doses normalised this parameter (*P*<0.05); effects of styrylcarbatone and metcarbatone were not significant (Table 2). In the heart, the expression of histone was observed mostly in the nuclei of cardiomyocytes, to a lesser extent it was also seen in the nuclei of interstitial inflammatory cells and endocardium (not shown). Development of DM increased the number of histone H2AX positive cells in triplicate (*P*=0.005). Treatment with etcabatone at both doses enhanced this increase (*P*<0.001). Metcarbatone at high dose decreased (*P*=0.038) the expression of H2AX in the nerve of intact rats but no other difference between the groups was observed in nerve and eye tissues (Table 3).

iNOS (*NOS2*) enzyme and *iNos* (*Nos2*) gene

Numerical data are presented in Tables 4 and 5. In kidneys, *iNOS* protein was expressed in glomeruli, canaliculi, stroma, and endothelium of blood vessels (not shown). Induction of diabetes caused a four-fold increase in the number of *iNOS*-positive cells (*P*=0.002), etcabatone

at low dose significantly decreased the expression (*P*=0.001) (Table 5), metcarbatone at low dose caused further up-regulation (*P*<0.001). Strikingly, the effects of the compounds on gene expression level in kidneys were adverse (Table 4): the development of diabetes produced a less drastic increase in the intensity of gene transcription (*P*=0.044), etcabatone at both doses produced an increase in intact animals (*P*<0.01), and at low dose it increased (*P*=0.003) the rate of transcription triggered by DM development. A similar effect was produced by metcarbatone at both doses (*P*<0.001). An even stronger increase in gene transcription was observed in blood cells (*P*=0.001), however, etcabatone at both doses (*P*=0.003) and metcarbatone at low dose (*P*=0.01) attenuated the effect of DM but styrylcarbatone did not produce any effect. Immunohistochemical analysis of heart tissues revealed the expression of *iNOS* in cardiomyocytes, inflammatory cells, blood vessel walls, and stroma. The enzyme was detected in pericardium and endocardium but predominant expression was observed in myocardium (not shown). In DM model, the enzyme expression increased four-fold compared to the control group (*P*=0.003; Table 5). A significant decrease in the effect was produced only by etcabatone at low dose (*P*=0.007). In the nerve, *iNOS*

Table 3 Effects of carbatonides on expression of DNA repair and apoptosis related proteins in control and diabetic rats

	Heart, c-PARP1	Heart, H2AX	Nerve, c-PARP1	Nerve, H2AX	Eye, c-PARP1	Eye, H2AX	Kidney, c-PARP1	Kidney, H2AX
Control	10.20±1.56 n=5	11.40±2.60 n=5	10.00±1.41 n=5	8.20±1.74 n=5	11.40±2.60 n=5	5.00±0.45 n=5	11.80±1.28 n=5	7.00±0.89 n=5
STZ	37.60±7.95 n=5*	32.80±4.48 n=5**	32.20±4.88 n=5**	6.60±2.01 n=5	32.80±4.48 n=5**	3.00±1.14 n=5	45.40±6.06 n=5**	11.00±1.55 n=5
Metcarbatone 0.05 mg kg ⁻¹	11.80±2.35 n=5	9.00±1.27 n=5	18.60±2.69 n=5	4.60±0.98 n=5	9.00±1.27 n=5	6.40±1.75 n=5	16.40±1.91 n=5	8.20±2.33 n=5
Metcarbatone 0.5 mg kg ⁻¹	9.20±1.20 n=5	12.20±0.20 n=5	15.40±2.11 n=5	3.60±0.75 n=5*	12.20±0.20 n=5	6.60±1.50 n=5	18.60±3.93 n=5	5.40±1.33 n=5
Metcarbatone 0.05 mg kg ⁻¹ + STZ	18.00±2.26 n=5#	29.40±4.23 n=5	33.00±9.46 n=5	3.40±1.03 n=5	29.40±4.23 n=5	5.20±0.97 n=5	55.60±10.91 n=5	8.67±2.57 n=6
Metcarbatone 0.5 mg kg ⁻¹ + STZ	25.60±8.26 n=5	28.60±6.02 n=5	18.40±3.98 n=5	4.00±0.84 n=5	28.60±6.02 n=5	3.80±0.66 n=5	37.60±6.42 n=5	7.80±1.83 n=5
Etcarbatone 0.05 mg kg ⁻¹	21.00±4.52 n=5	13.80±1.80 n=5	24.80±5.95 n=5*	7.60±1.72 n=5	13.80±1.80 n=5	6.20±2.60 n=5	25.40±3.75 n=5*	6.80±0.86 n=5
Etcarbatone 0.5 mg kg ⁻¹	8.20±1.16 n=5	15.80±3.80 n=5	17.20±1.96 n=5	6.40±4.23 n=5	15.80±3.80 n=5	6.80±3.93 n=5	28.20±4.53 n=5*	6.40±1.81 n=5
Etcarbatone 0.05 mg kg ⁻¹ + STZ	10.80±1.74 n=5###	75.00±6.36 n=5###	7.400±1.47 n=5###	4.20±1.11 n=5	75.00±6.36 n=5###	5.20±2.06 n=5	10.20±1.46 n=5###	33.00±4.62 n=5###
Etcarbatone 0.5 mg kg ⁻¹ + STZ	19.40±3.83 n=5##	66.80±5.86 n=5###	10.60±3.37 n=5###	6.80±3.61 n=5	66.80±5.86 n=5###	5.40±1.91 n=5	20.40±4.08 n=5###	40.00±8.12 n=5###

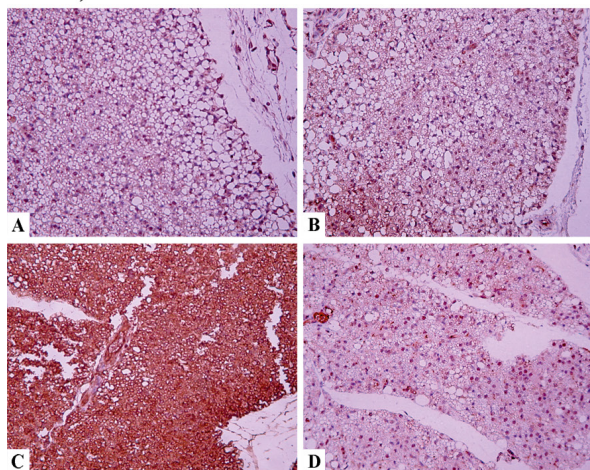
STZ – streptozotocin. Values are represented as the mean ± SEM. **p*<0.05; ***p*<0.01; ****p*<0.001 vs. Control. #*p*<0.05; ##*p*<0.01; ###*p*<0.001 vs. STZ

expression was observed in Schwann's cells (Figure 4); it increased in diabetic rats ($P=0.003$). A low dose of etcarbatone increased the expression in control rats ($P<0.001$), while both doses of etcarbatone decreased it in diabetic animals ($P<0.05$). Development of DM caused qualitative changes in the distribution of iNOS-positive cells in eye tissues: in the eyes of intact animals the expression was detected mostly in the ciliary body, while in diabetic animals iNOS positive cells were observed also in the retina and vitreous body. The general number of positive cells also increased (Figure 4). Quantitatively, induction of diabetes increased iNOS expression ($P=0.021$) but the compounds did not modify the expression significantly (Table 5).

eNOS (NOS3) enzyme and eNos (Nos3) gene

Data are presented in Tables 4 and 5. In heart tissues, eNOS expression was observed in the cytoplasm of

iNOS, sciatic nerve



iNOS, eye

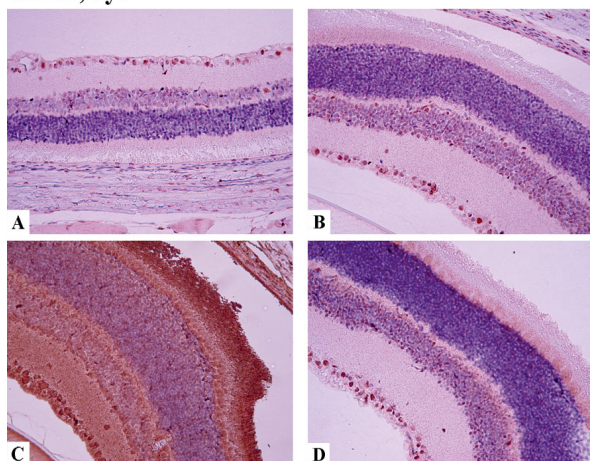


Figure 4 Tissue distribution of iNOS in organs of normal and diabetic rats. Upper panel: iNOS expression in the sciatic nerve tissue. Immunohistochemical staining method, magnification $\times 200$. A - control, B - etcarbatone at 0.5 mg kg^{-1} , C - STZ (streptozotocin), D - STZ+etcarbatone 0.5 mg kg^{-1} . Lower panel: iNOS expression in eye's tissue. Immunohistochemical staining method, magnification $\times 200$. A - control, B - etcarbatone at 0.5 mg kg^{-1} , C - STZ, D - STZ+etcarbatone at 0.5 mg kg^{-1}

cardiomyocytes and inflammatory cells and in endothelium (not shown). We could not detect significant differences between control and STZ group, however, etcarbatone treatment at both doses up-regulated the protein expression in the heart of diabetic animals ($P<0.001$). In kidney tissues, the enzyme was expressed in the cytoplasm of the cells forming proximal and distal canaliculi and in endothelium (not shown). Development of *diabetes mellitus* decreased the enzyme expression in kidneys compared to controls ($P<0.001$). The expression was up-regulated by a low dose of metcarbatone ($P=0.016$) and both doses of etcarbatone ($P<0.001$, Table 5). In nerve cells, eNOS protein expression increased by induction of diabetes ($P=0.008$). It was normalised by both doses of etcarbatone ($P<0.01$). In the eyes of intact animals, the expression of eNOS was restricted to the ciliary body; on the contrary, in diabetic animals it was observed not only in the ciliary body, but also in the retina, vitreous body, and inflammatory cells (not shown). Qualitative expansion of the expression was followed also by a numerical increase in eNOS-positive cells ($P<0.001$).

The expression of *eNos* gene decreased in the kidneys of diabetic animals ($P=0.04$, Table 4). Both etcarbatone and metcarbatone at high doses increased the expression levels ($P=0.009$ and $P=0.024$, respectively). Styrylcarbatone decreased gene expression by high dose in intact animals ($P=0.019$) and by low dose in diabetic rats ($P=0.024$).

Xanthine deoxygenase gene (Xdh)

Formerly we have demonstrated that the overall increase in NO production in STZ model of DM was due in part to NOS-independent production of NO by xanthine deoxygenase (10). Therefore, it was interesting to monitor the expression of this gene. Surprisingly, the increase in gene expression was detected only in the blood of diabetic animals ($P=0.006$; Table 4); styrylcarbatone and etcarbatone decreased it significantly (styrylcarbatone: $P=0.02$ for low dose; etcarbatone: $P=0.003$ for low dose, and $P=0.001$ for high dose). In kidneys, diabetes development did not change the expression of the gene, however, metcarbatone and styrylcarbatone up-regulated its expression in the kidneys of both control (metcarbatone: $P=0.04$ for low dose, $P=0.003$ for high dose; styrylcarbatone: $P<0.001$ for both doses) and diabetic animals (metcarbatone: $P<0.001$ for both doses, styrylcarbatone: $P<0.001$ for high dose). Etcarbatone produced similar effects; in the control group, it increased the expression of *Xdh* gene in the kidneys ($P<0.001$ for both doses). In diabetic animals, both concentrations of etcarbatone up-regulated gene expression ($P=0.001$ for low dose and $P=0.015$ for high dose).

Comet assay

Development of *diabetes mellitus* increased the level of DNA breakage in white blood cells ($P<0.001$, Figure 5). Surprisingly, metcarbatone, etcarbatone, and styrylcarbatone

Table 4 Effects of carbatonides on expression of iNos and Xdh genes in kidneys and blood of control and diabetic rats

	Kidneys, iNos	Kidneys, eNos	Kidneys, Xdh	Blood, iNos	Blood, Xdh
Control	0.0016±0.0002 n=11	0.0106±0.0014 n=11	1.39±0.11 n=11	0.018±0.004 n=11	0.31±0.04 n=11
STZ	0.0035±0.0006 n=13**	0.0071±0.0005 n=12*	1.78±0.27 n=13	0.063±0.011 n=15**	0.58±0.08 n=15**
Metcarbatone 0.05 mg kg ⁻¹	0.0024±0.0003 n=4	0.0089±0.0009 n=4	2.04±0.11 n=4	0.015±0.003 n=4	0.29±0.05 n=4
Metcarbatone 0.5 mg kg ⁻¹	0.0024±0.0006 n=4	0.0094±0.0015 n=4	2.38±0.21 n=4	0.012±0.002 n=4	0.17±0.02 n=4
Metcarbatone 0.05 mg kg ⁻¹ + STZ	0.0061±0.0002 n=5 [#]	0.0086±0.0012 n=5	2.60±0.24 n=5	0.018±0.002 n=4*	0.35±0.06 n=4
Metcarbatone 0.5 mg kg ⁻¹ + STZ	0.0074±0.0013 n=5 ^{###}	0.0126±0.0036 n=5 [#]	3.35±0.54 n=5 ^{###}	0.042±0.012 n=5	0.41±0.08 n=5
Etcarbatone 0.05 mg kg ⁻¹	0.0042±0.0008 n=3*	0.0109±0.0022 n=3	2.43±0.30 n=3*	0.019±0.004 n=3	0.25±0.05 n=3
Etcarbatone 0.5 mg kg ⁻¹	0.0038±0.0004 n=4*	0.0069±0.0005 n=4	2.57±0.25 n=4**	0.010±0.002 n=4	0.24±0.03 n=4
Etcarbatone 0.05 mg kg ⁻¹ + STZ	0.0045±0.0003 n=5	0.0092±0.0017 n=5	1.89±0.13 n=5	0.013±0.004 n=4 ^{##}	0.28±0.09 n=5 ^{##}
Etcarbatone 0.5 mg kg ⁻¹ + STZ	0.0023±0.0004 n=5	0.0131±0.0026 n=5 ^{##}	1.71±0.20 n=5	0.014±0.001 n=5 ^{##}	0.19±0.01 n=5 ^{##}
Styrylcarbatone 0.05 mg kg ⁻¹	0.0029±0.0001 n=4	0.0095±0.0021 n=4	2.55±0.26 n=4*	0.016±0.005 n=4	0.28±0.08 n=4
Styrylcarbatone 0.5 mg kg ⁻¹	0.0021±0.0002 n=3	0.0058±0.0008 n=4*	2.45±0.10 n=3*	0.022±0.004 n=3	0.32±0.08 n=3
Styrylcarbatone 0.05 mg kg ⁻¹ + STZ	0.0035±0.0005 n=5	0.0030±0.0004 n=5 [#]	1.58±0.15 n=5	0.050±0.016 n=5	0.28±0.08 n=5 [#]
Styrylcarbatone 0.5 mg kg ⁻¹ + STZ	0.0036±0.0005 n=5	0.0103±0.0007 n=5	2.72±0.27 n=5 [#]	0.074±0.033 n=4	0.42±0.05 n=4

STZ – streptozotocin. Values are represented as the mean ± SEM. **p*<0.05; ***p*<0.01; ****p*<0.001 vs. Control. [#]*p*<0.05; ^{##}*p*<0.01; ^{###}*p*<0.001 vs. STZ

increased the level of DNA breakage in intact animals ($P<0.05$); etcarbatone at high dose drastically increased DNA lesions also in diabetic animals ($P<0.001$). However, metcarbatone at high dose ($P<0.001$) and styrylcarbatone at low dose ($P=0.041$) alleviated DNA damage level.

DISCUSSION

In the present study, we have performed *in vitro* and *in vivo* assays of several physicochemical properties and biological activities of carbatonides [disodium-2,6-dimethyl-1,4-dihydropyridine-3,5-bis(carbonyloxyacetate) derivatives]. Our aim was to evaluate a probable use of these compounds for treating DM complications. It turned out that replacing groups in position 4 could drastically modify the hydroxyl radical scavenging capability of the compounds; metcarbatone was much more effective compared to other compounds. Indeed, former studies indicate that radical-scavenging activity is really determined by position 4; a free carboxylic group in this position is considered to be the most favourable for radical scavenging. Our study shows that methyl group in this position also favours effective scavenging, at least under conditions of the chosen assay. However, radical scavenging activity of 1,4-DHPs strongly depends on the used system (4). Besides position 4, the tested compounds were identical, thus, the considerations that electron donor substituents in positions 2 and 6 promote the quenching of oxidation, as well as stronger electron acceptors in positions 3 and 5 (4) cannot be applied to this study. All five compounds were capable of interacting with DNA, although their affinity to DNA was lower compared to other 1,4-DHPs (10, 12). The increase in fluorescence of carbatone and propcarbatone in the presence of DNA indicates a probable intercalation mechanism; the quenching of fluorescence by metcarbatone and etcarbatone indicates binding to the outer surface of

DNA molecule (18). Interestingly, styrylcarbatone manifested a higher affinity to DNA, although DNA quenched its fluorescence, ethidium bromide extrusion assay indicates intercalation. The compound might interact with DNA via two mechanisms – intercalation and minor groove binding. Probably, direct interactions of styrylcarbatone, etcarbatone, and metcarbatone with DNA are responsible for DNA damage in white blood cells of the intact animals observed after the administration of these compounds. DNA-damaging effects of antioxidant compounds are a frequently observed phenomenon, for example, antioxidant flavonoids induce oxidative DNA damage serving as temporary carriers of electrons received from transition metal ions that are relayed to oxygen molecules to subsequently generate superoxide and H_2O_2 (19). The DNA break reducing effect of metcarbatone in diabetic animals appears to be due to the radical scavenging activity of the compound, the weak scavenger etcarbatone even worsens the situation. This might be the cause of the increase in *Parp1* gene expression in intact animals as a consequence of a triggered DNA repair process.

The gene and protein expression studies revealed several effects of these compounds, which appear to be benevolent in condition of *diabetes mellitus*. Coherent up-regulation of both mRNA and protein of eNOS in the kidneys of diabetic animals triggered by both metcarbatone and etcarbatone appears to be a promising effect. In the myocardium, the decrease in the eNOS protein expression was not pronounced, still etcarbatone up-regulated it in diabetic animals. The uncoupling of the endothelial NO synthase with consequent production of superoxide radical and decrease in NO bioavailability is an important factor in the pathogenesis of complications of DM (20). To heal the complications, the uncoupling should be pharmacologically reduced (21) but eNOS protein expression should be stimulated; its activity should be

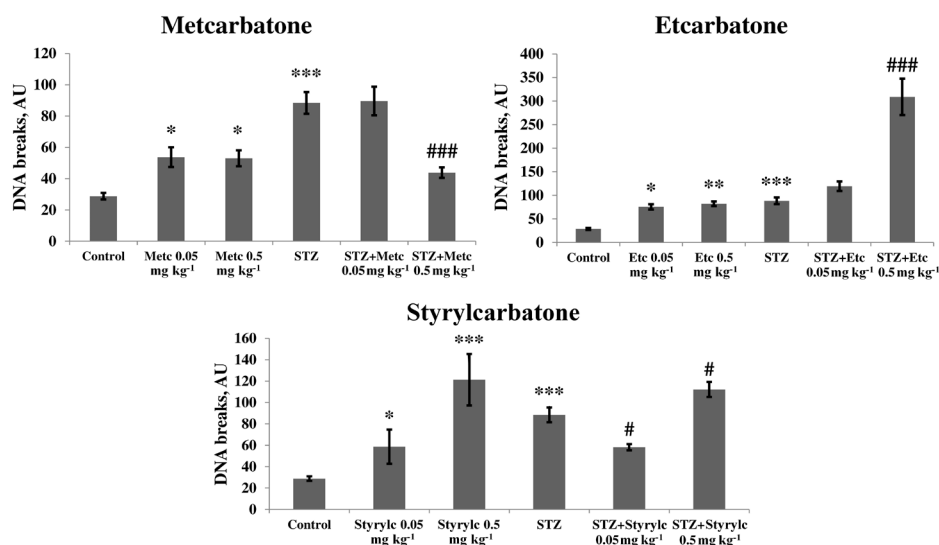


Figure 5 Effects of carbatonides on DNA integrity in white blood cells of normal and diabetic rats. STZ – streptozotocin; $n=3-17$. Values are represented as the mean \pm SEM. * $p<0.05$; ** $p<0.01$; *** $p<0.001$ vs. Control. # $p<0.05$; ### $p<0.001$ vs. STZ

Table 5 Effects of carbatonides on expression of NO synthases in control and diabetic rats

	Heart, iNOS	Heart, eNOS	Nerve, iNOS	Nerve, eNOS	Eye, iNOS	Eye, eNOS	Kidney, iNOS	Kidney, eNOS
Control	7.50±1.71 n=4	13.20±0.58 n=5	5.60±1.17 n=5	9.00±1.73 n=5	5.80±2.01 n=5	9.00±1.26 n=5	8.80±1.16 n=5	12.20±0.49 n=5
STZ	29.67±4.55 n=6**	11.00±3.33 n=5	21.20±2.82 n=5***	22.00±2.97 n=5**	14.40±2.20 n=5*	24.20±1.11 n=5***	31.38±4.72 n=8**	3.20±0.73 n=5***
Metcarbatone 0.05 mg kg ⁻¹	15.60±1.40 n=5	8.40±1.50 n=5	7.60±1.29 n=5	5.60±1.81 n=5	7.00±2.49 n=5	10.20±5.32 n=5	22.40±2.82 n=5	8.60±1.08 n=5
Metcarbatone 0.5 mg kg ⁻¹	13.00±1.34 n=5	12.00±3.02 n=5	6.20±1.28 n=5	7.80±2.40 n=5	5.80±1.02 n=5	7.00±1.34 n=5	17.00±1.73 n=5	13.00±5.04 n=5
Metcarbatone 0.05 mg kg ⁻¹ + STZ	35.17±4.35 n=6	10.83±1.45 n=6	22.00±1.05 n=5	24.60±4.59 n=5	14.00±2.97 n=5	26.40±3.92 n=5	56.86±7.39 n=7###	13.00±2.76 n=5#
Metcarbatone 0.5 mg kg ⁻¹ + STZ	32.50±3.21 n=6	11.20±5.98 n=5	18.20±1.88 n=5	20.80±5.91 n=5	12.60±0.87 n=5	26.20±2.40 n=5	29.57±4.59 n=7	5.40±0.51 n=5
Etcarbatone 0.05 mg kg ⁻¹	17.20±2.18 n=5	8.20±1.93 n=5	21.60±1.94 n=5***	6.00±1.23 n=5	7.60±2.02 n=5	6.60±1.50 n=5	22.43±4.31 n=7	10.80±0.73 n=5
Etcarbatone 0.5 mg kg ⁻¹	10.00±0.89 n=5	11.00±1.55 n=5	9.20±1.32 n=5	9.80±1.88 n=5	13.00±0.77 n=5	14.20±6.12 n=5	13.80±2.20 n=5	10.20±0.97 n=5
Etcarbatone 0.05 mg kg ⁻¹ + STZ	11.17±2.09 n=6###	51.20±4.05 n=5###	9.40±0.68 n=5###	9.60±1.03 n=5###	7.80±1.02 n=5	18.60±7.06 n=5	12.13±2.96 n=8#	26.20±3.96 n=5###
Etcarbatone 0.5 mg kg ⁻¹ + STZ	20.83±4.76 n=6	46.80±13.40 n=5###	15.20±1.36 n=5#	13.40±0.87 n=5###	17.00±4.24 n=5	15.40±4.65 n=5	25.00±4.36 n=8	23.00±5.49 n=5###

STZ – streptozotocin. Values are represented as the mean ± SEM. *p<0.05; **p<0.01; ***p<0.001 vs. Control. #p<0.05; ##p<0.01; ###p<0.001 vs. STZ

increased (22, 23). Up-regulation of eNOS favours sensitivity to insulin (24). Recent data indicate an important role of the regulation of eNOS expression in many processes, despite its “constitutive” nature (25). Thus, metcarbatone and etcarbatone appear to produce favourable effects aimed at preventing diabetic nephropathy and cardiomyopathy. However, our results on the eNOS expression in eye tissues contradict the published data, as a decrease in eNOS in diabetic retina was observed by others (26). It seems that the problem should be studied more in detail. A similar effect was observed in the sciatic nerve, eNOS was up-regulated in diabetic animals, etcarbatone down-regulated its expression. Our data contradict the findings of others (27) indicating a decrease in *eNos* expression in the sciatic nerve of mice predisposed to development of DM and an increase in expression as a result of the applied therapy. However, our model of DM was different and nerve tissue might have its peculiarities. For example, a simultaneous increase in iNOS and eNOS was observed in the hippocampus of animals subjected to hypoxia (28). On the contrary, in the paraventricular nucleus of animals with modelled insulin resistance, eNOS was down-regulated; expression of iNOS did not change (29). Others have also shown an increased as well as decreased expression of eNOS in different tissues of diabetic animals (30).

The observed increase in iNOS protein and *iNos* gene in the studied tissues of diabetic animals was in good correlation with published data. The increase in iNOS expression coupled to DM was reported for cardiomyocytes (31), blood vessels (32), retina (26), sciatic nerve (27) and kidneys (10). The ability to decrease iNOS expression is considered to be a positive feature in the search for remedies which are aimed to treat diabetes complications (33). Etcarratone appears to be prospective from this point of view, as it reduced the expression of iNOS protein in heart, nerve, and kidney tissues, metcarbatone was ineffective. Concerning *iNos* gene expression, it was drastically up-regulated in the kidneys of intact animals by styrylcarbatone and etcarbatone, stronger than in the DM model, and also up-regulated by metcarbatone and etcarbatone in diabetic animals. In blood, the increase in the *iNos* gene expression was triggered by the development of DM, and etcarbatone and metcarbatone normalised it. Thus, the effects on iNOS protein and gene expression are not coherent. This can be explained by the mechanisms of gene regulation: it is regulated post-transcriptionally to a large extent, maintenance of mRNA stability being very important (34, 35). The consequences of the observed outburst of mRNA expression could be levelled by post-transcriptional processing. Expression of the *Parp1* gene related to DNA repair and induced by DNA breakage resembled to a large extent the pattern of the *iNos* gene expression, co-ordinate expression of these genes is due to common Nrf-2 pathway of their regulation (36, 37). Thus, 1,4-DHPs increased the expression of the gene in kidneys of both intact and diabetic

animals. 1,4-DHPs *per se* did not increase gene expression in blood, but etcarbatone attenuated the DM-triggered increase. Interestingly, the effects on *Xdh* gene expression were similar; the enzyme contributes to a large extent to NOS-independent NO production. Surprisingly, these data are in contradiction with the level of DNA breakage – metcarbatone decreased it in diabetic animals but etcarbatone increased it. The marker of DNA double-strand breaks, the H2AX histone, did not react on DM induction in kidneys neither at gene, nor at protein expression levels. Surprisingly, etcarbatone up-regulated the expression of the protein, indicating the generation of double-strand DNA breaks. Discrepancy between mRNA and protein expression is not surprising, as the antibody detects the phosphorylated form of histone, generated after translation. It is phosphorylated by kinases such as ataxia telangiectasia mutated and ataxia telangiectasia mutated-Rad3-related in the PI3K pathway (38). However, we did observe an increased expression of the gene in blood cells, coherent with DNA breakage increase; perhaps, this reflects the fact that in lymphocytes the non-phosphorylated form of histone is also translocated to DNA breakage foci (39) triggering an increased transcription of the gene by feedback mechanism. Etcarratone up-regulated also H2AX histone in myocardium. DNA double-strand breaks are usually associated with final stages of apoptosis; it was interesting to compare data on histone H2AX expression and generation of cleaved PARP1, a marker of apoptosis. In kidneys, DM triggered a sharp increase in the c-PARP1 production; interestingly, etcarbatone treatment produced a strong anti-apoptotic effect. Thus, the DNA double-strand breaks produced by the compound should be repaired. The effects in myocardium were similar, again etcarbatone produced an anti-apoptotic effect, and thus H2AX expression indicates the generation of reparable double-strand breaks formed prior to apoptosis. Action of etcarbatone in the sciatic nerve is also anti-apoptotic; unfortunately, it is pro-apoptotic in eye tissues.

Taken together, our data indicate that derivatives of disodium-2,6-dimethyl-1,4-dihydropyridine-3,5-bis(carboxyloxyacetate) appear to be a prospective compound group for the development of drugs aimed to treat DM complications like diabetic nephropathy, cardiomyopathy, and neuropathy. Etcarratone appears to be the most prospective due to its ability to down-regulate iNOS, up-regulate eNOS, and prevent apoptosis in kidneys, hearts, and nerves of organisms suffering of hyperglycaemia.

Acknowledgements

This work was supported by the National Research Programme “Biomedicine 2014”.

Conflict of interest

The authors declare that they have no conflict of interest.

Abbreviations

1,4-DHP	1,4-dihydropyridine
c-PARP1	cleaved poly [ADP-ribose] polymerase 1
D	DNA damage
DM	<i>diabetes mellitus</i>
DMPO	5,5-dimethylpyrroline- <i>N</i> -oxide
DMSO	dimethyl sulfoxide
EDTA	ethylenediaminetetraacetic acid
eNOS	endothelial nitric oxide synthase
EPR	electron paramagnetic resonance
ESR	electron spin resonance
G	gauss
<i>H2afx</i>	H2A histone family member X, gene
H2AX	H2A histone family member X, protein
iNOS	inducible nitric oxide synthase
mRNA	messenger RNA
NaCl	sodium chloride
NaOH	sodium hydroxide
NO	nitric oxide
PARP1	poly [ADP-ribose] polymerase 1
PBS	phosphate-buffered saline
PCR	polymerase chain reaction
PI3K	phosphoinositide 3-kinase
<i>p.o.</i>	<i>per os</i>
SEM	standard error of the mean
STZ	streptozotocin
T1DM	type one <i>diabetes mellitus</i>
UK	United Kingdom
USA	United States of America
UV/VIS	ultraviolet-visible
XDH	xanthine deoxygenase

REFERENCES

1. Chen X, Tang J, Xie W, Wang J, Jin J, Ren J, Jin L, Lu J. Protective effect of the polysaccharide from *Ophiopogon japonicus* on streptozotocin-induced diabetic rats. *Carbohydr Polym* 2013;94:378-85. doi: 10.1016/j.carbpol.2013.01.037
2. Fu H, Li G, Liu C, Li J, Wang X, Cheng Liu T. Probucol prevents atrial remodeling by inhibiting oxidative stress and TNF- α /NF- κ B/TGF- β signal transduction pathway in alloxan-induced diabetic rabbits. *J Cardiovasc Electrophysiol* 2015;26:211-22. doi: 10.1111/jce.12540
3. Drigelová M, Tarabová B, Duburs G, Lacinová L. The dihydropyridine analogue cerebrocrast blocks both T-type and L-type calcium currents. *Can J Physiol Pharmacol* 2009;87:923-32. doi: 10.1139/y09-086
4. Velená A, Zarkovic N, Gall Troselj K, Bisenieks E, Krauze A, Poikāns J, Duburs G. 1,4-Dihydropyridine derivatives: dihydronicotinamide analogues-model compounds targeting oxidative stress. *Oxid Med Cell Longev* 2016;2016:1892412. doi: 10.1155/2016/1892412
5. Fernandes MA, Pereira SP, Jurado AS, Custódio JB, Santos MS, Moreno AJ, Duburs G, Vicente JA. Comparative effects of three 1,4-dihydropyridine derivatives [OSI-1210, OSI-1211 (etaftoron), and OSI-3802] on rat liver mitochondrial bioenergetics and on the physical properties of membrane

- lipid bilayers: relevance to the length of the alkoxy chain in positions 3 and 5 of the DHP ring. *Chem Biol Interact* 2008;173:195-204. doi: 10.1016/j.cbi.2008.03.001
6. Briede J, Stivrina M, Stoldere D, Vigante B, Duburs G. Effect of cerebrocrast on body and organ weights, food and water intake, and urine output of normal rats. *Cell Biochem Funct* 2008;26:908-15. doi: 10.1002/cbf.1525
7. Briede J, Stivriņa M, Stoldere D, Bisenieks E, Uldriķis J, Poikāns J, Makarova N, Duburs G. Effect of new and known 1,4-dihydropyridine derivatives on blood glucose levels in normal and streptozotocin-induced diabetic rats. *Cell Biochem Funct* 2004;22:219-24. doi: 10.1002/cbf.1091
8. Briede J, Stivrina M, Stoldere D, Vigante B, Duburs G. Effect of cerebrocrast, a new long-acting compound on blood glucose and insulin levels in rats when administered before and after STZ-induced diabetes mellitus. *Cell Biochem Funct* 2007;25:673-80. doi: 10.1002/cbf.1372
9. Briede J, Stivrina M, Vigante B, Stoldere D, Duburs G. Acute effect of antidiabetic 1,4-dihydropyridine compound cerebrocrast on cardiac function and glucose metabolism in the isolated, perfused normal rat heart. *Cell Biochem Funct* 2008;26:238-45. doi: 10.1002/cbf.1442
10. Leonova E, Sokolovska J, Boucher JL, Isajevs S, Rostoka E, Baumane L, Sjakste T, Sjakste N. New 1,4-dihydropyridines down-regulate nitric oxide in animals with streptozotocin-induced diabetes mellitus and protect deoxyribonucleic against peroxynitrite action. *Basic Clin Pharmacol Toxicol* 2016;119:19-31. doi: 10.1111/bcpt.12542
11. Ryabokon NI, Goncharova RI, Duburs G, Rzeszowska-Wolny J. A 1,4-dihydropyridine derivative reduces DNA damage and stimulates DNA repair in human cells *in vitro*. *Mutat Res* 2005;587:52-8. doi: 10.1016/j.mrgentox.2005.07.009
12. Buraka E, Chen CY, Gavare M, Grube M, Makarenkova G, Nikolajeva V, Bisenieks I, Brūvere I, Bisenieks E, Duburs G, Sjakste N. DNA-binding studies of AV-153, an antimutagenic and DNA repair-stimulating derivative of 1,4-dihydropyridine. *Chem Biol Interact* 2014;220:200-7. doi: 10.1016/j.cbi.2014.06.027
13. Ošiča K, Rostoka E, Isajevs S, Sokolovska J, Sjakste T, Sjakste N. Effects of an antimutagenic 1,4-dihydropyridine AV-153 on expression of nitric oxide synthases and DNA repair-related enzymes and genes in kidneys of rats with a streptozotocin model of diabetes mellitus. *Basic Clin Pharmacol Toxicol* 2016;119:458-63. doi: 10.1111/bcpt.12617
14. Ošiča K, Rostoka E, Sokolovska J, Paramonova N, Bisenieks E, Duburs G, Sjakste N, Sjakste T. 1,4-Dihydropyridine derivatives without Ca²⁺-antagonist activity up-regulate Psm6 mRNA expression in kidneys of intact and diabetic rats. *Cell Biochem Funct* 2016;34:3-6. doi: 10.1002/cbf.3160
15. Chen W, Feng L, Huang Z, Su H. Hispidin produced from *Phellinus linteus* protects against peroxynitrite-mediated DNA damage and hydroxyl radical generation. *Chem Biol Interact* 2012;199:137-42. doi: 10.1016/j.cbi.2012.07.001
16. Tice RR, Agurell E, Anderson D, Burlinson B, Hartmann A, Kobayashi H, et al. Single cell gel/comet assay: guidelines for *in vitro* and *in vivo* genetic toxicology testing. *Environ Mol Mutagen* 2000;35:206-21. doi: 10.1002/(SICI)1098-2280(2000)35:3<206::AID-EM8>3.0.CO;2-J

17. Olive PL, Banáth JP. The comet assay: a method to measure DNA damage in individual cells. *Nat Protoc* 2006;1:23-9. doi: 10.1038/nprot.2006.5
18. Na N, Zhao DQ, Li H, Jiang N, Wen JY, Liu HY. DNA binding, photonuclease activity and human serum albumin interaction of a water-soluble freebase carboxyl corrole. *Molecules*. 2015;21(1):pii:E54. DOI: 10.3390/molecules21010054.
19. Tsai YC, Wang YH, Liou CC, Lin YC, Huang H, Liu YC. Induction of oxidative DNA damage by flavonoids of propolis: its mechanism and implication about antioxidant capacity. *Chem Res Toxicol* 2012;25:191-6. doi: 10.1021/tx200418k
20. Takahashi T, Harris RC. Role of endothelial nitric oxide synthase in diabetic nephropathy: lessons from diabetic eNOS knockout mice. *J Diabetes Res* 2014;2014:590541. doi: 10.1155/2014/590541
21. Roe ND, Ren J. Nitric oxide synthase uncoupling: a therapeutic target in cardiovascular diseases. *Vascul Pharmacol* 2012;57:168-72. doi: 10.1016/j.vph.2012.02.004
22. Liu B, Kuang L, Liu J. Bariatric surgery relieves type 2 diabetes and modulates inflammatory factors and coronary endothelium eNOS/iNOS expression in db/db mice. *Can J Physiol Pharmacol* 2014;92:70-7. doi: 10.1139/cjpp-2013-0034
23. Förstermann U, Li H. Therapeutic effect of enhancing endothelial nitric oxide synthase (eNOS) expression and preventing eNOS uncoupling. *Br J Pharmacol* 2011;164:213-23. doi: 10.1111/j.1476-5381.2010.01196.x
24. Perdomo L, Beneit N, Otero YF, Escribano Ó, Díaz-Castroverde S, Gómez-Hernández A, Benito M. Protective role of oleic acid against cardiovascular insulin resistance and in the early and late cellular atherosclerotic process. *Cardiovasc Diabetol* 2015;14:75. doi: 10.1186/s12933-015-0237-9
25. Mattila JT, Thomas AC. Nitric oxide synthase: non-canonical expression patterns. *Front Immunol* 2014;5:478. doi: 10.3389/fimmu.2014.00478
26. Zhang L, Dong L, Liu X, Jiang Y, Zhang L, Zhang X, Li X, Zhang Y. α -Melanocyte-stimulating hormone protects retinal vascular endothelial cells from oxidative stress and apoptosis in a rat model of diabetes. *PLoS One* 2014;9:e93433. doi: 10.1371/journal.pone.0093433
27. Chen YL, Chen KH, Yin TC, Huang TH, Yuen CM, Chung SY, Sung PH, Tong MS, Chen CH, Chang HW, Lin KC, Ko SF, Yip HK. Extracorporeal shock wave therapy effectively prevented diabetic neuropathy. *Am J Transl Res* 2015;7:2543-60. PMID: PMC4731656
28. Huang CC, Lai CJ, Tsai MH, Wu YC, Chen KT, Jou MJ, Fu PI, Wu CH, Wei IH. Effects of melatonin on the nitric oxide system and protein nitration in the hypobaric hypoxic rat hippocampus. *BMC Neurosci* 2015;16:61. doi: 10.1186/s12868-015-0199-6
29. Lu QB, Feng XM, Tong N, Sun HJ, Ding L, Wang YJ, Wang X, Zhou YB. Neuronal and endothelial nitric oxide synthases in the paraventricular nucleus modulate sympathetic overdrive in insulin-resistant rats. *PLoS One* 2015;10(10):e0140762. doi: 10.1371/journal.pone.0140762
30. Heltianu C, Guja C. Role of nitric oxide synthase family in diabetic neuropathy. *J Diabetes Metab* 2011;S5:002. doi: 10.4172/2155-6156.S5-002
31. Puthanveetil P, Zhang D, Wang Y, Wang F, Wan A, Abrahani A, Rodrigues B. Diabetes triggers a PARP1 mediated death pathway in the heart through participation of FoxO1. *J Mol Cell Cardiol* 2012;53:677-86. doi: 10.1016/j.yjmcc.2012.08.013
32. Martínez AC, Hernández M, Novella S, Martínez MP, Pagán RM, Hermenegildo C, García-Sacristán A, Prieto D, Benedito S. Diminished neurogenic femoral artery vasoconstrictor response in a Zucker obese rat model: differential regulation of NOS and COX derivatives. *PLoS One* 2014;9(9):e106372. doi: 10.1371/journal.pone.0106372
33. Ahad A, Mujeeb M, Ahsan H, Siddiqui WA. Prophylactic effect of baicalein against renal dysfunction in type 2 diabetic rats. *Biochimie* 2014;106:101-10. doi: 10.1016/j.biochi.2014.08.006
34. Pautz A, Art J, Hahn S, Nowag S, Voss C, Kleinert H. Regulation of the expression of inducible nitric oxide synthase. *Nitric Oxide* 2010;23:75-93. doi: 10.1016/j.niox.2010.04.007
35. Casper I, Nowag S, Koch K, Hubrich T, Bollmann F, Henke J, Schmitz K, Kleinert H, Pautz A. Post-transcriptional regulation of the human inducible nitric oxide synthase (iNOS) expression by the cytosolic poly(A)-binding protein (PABP). *Nitric Oxide* 2013;33:6-17. doi: 10.1016/j.niox.2013.05.002
36. Perrotta I, Brunelli E, Sciangula A, Conforti F, Perrotta E, Tripepi S, Donato G, Cassese M. iNOS induction and PARP-1 activation in human atherosclerotic lesions: an immunohistochemical and ultrastructural approach. *Cardiovasc Pathol* 2011;20:195-203. doi: 10.1016/j.carpath.2010.06.002
37. Chen B, Lu Y, Chen Y, Cheng J. The role of Nrf2 in oxidative stress-induced endothelial injuries. *J Endocrinol* 2015;225:R83-99. doi: 10.1530/JOE-14-0662
38. Kuo LJ, Yang LX. Gamma-H2AX - a novel biomarker for DNA double-strand breaks. *In Vivo* 2008;22:305-9. PMID: 18610740
39. Tchurikov NA, Yudkin DV, Gorbacheva MA, Kulemzina AI, Grisichenko IV, Fedoseeva DM, Sosin DV, Kravatsky YV, Kretova OV. Hot spots of DNA double-strand breaks in human rDNA units are produced *in vivo*. *Sci Rep* 2016;6:25866. doi: 10.1038/srep25866

Modifikacije ekspresije gena i proteina koji su uključeni u popravak DNA i metabolizam dušikova oksida karbonylidima [derivati dinatrij-2,6-dimetil-1,4-dihidropiridin-3,5-bis(karboniloksiacetata)] u kontrolnih i dijabetičkih štakora

Rezultati ispitivanja patogeneze komplikacija šećerne bolesti (*diabetes mellitus* – DM) upozoravaju na to da bi tvari koje smanjuju nastanak slobodnih radikala a pospješuju popravak DNA mogle biti obećavajuće u budućem liječenju te bolesti. U ovome su istraživanju ispitana navedena svojstva karbonylida, derivata dinatrij-2,6-dimetil-1,4-dihidropiridin-3,5-bis(karboniloksiacetata). EPR spektroskopija je pokazala da je metkarbaton učinkovit sakupljač hidroksilnih radikala koji nastaju Fentonovom reakcijom. Etkarbaton i propkarbaton su bili malo manje učinkoviti, a stirkarbaton nije bio učinkovit. UV/VIS spektroskopija pokazala je hiperkromni učinak stirkarbatona u interakciji s DNA, a svi ostali karbonylidi pokazali su hipokromni učinak. Štakori kod kojih je DM tipa 1 induciran streptozotocinom tretirani su metkarbatonom, etkarbatonom ili stirkarbatonom (sve tvari su davane u dozi 0,05 mg kg⁻¹ ili 0,5 mg kg⁻¹) tijekom devet dana nakon što je potvrđeno da je izazvan DM. Razine ekspresije gena u bubrezima procijenjene su kvantitativnim RT-PCR-om, ekspresija proteina – imunohistokemijski u bubrezima, srcu, ishijadičnom živcu i očima, a lom DNA – komet-testom bijelim krvnim stanicama. Indukcija DM-a uzrokovala je lomove u DNA; metkarbaton i stirkarbaton (niska doza) ublažili su ovaj učinak. Metkarbaton i etkarbaton pojačali su mRNA i ekspresiju proteina eNOS-a u bubrezima dijabetičkih životinja; etkarbaton je takav učinak pokazao i u miokardu. Etkarbaton je smanjio ekspresiju iNOS proteina u miokardu, živcu i bubrezima. Ekspresija iNOS-a bila je pojačana u bubrezima primjenom etkarbatona i metkarbatona u dijabetičkih životinja. Razvoj DM povećao je ekspresiju iNOS-a u krvi, a etkarbaton i metkarbaton vratili su ju na normalne vrijednosti. Etkarbaton je pojačao ekspresiju H2AX u bubrezima dijabetičkih životinja, ali je smanjio proizvodnju c-PARP1. Naši podaci upućuju na potencijal karbonylida kao lijekova za liječenje komplikacija uzrokovanih dijabetesom.

KLJUČNE RIJEČI: derivati 1,4-dihidropiridina; diabetes mellitus; DNA lom; sakupljači slobodnih radikala; sintaza dušikova oksida